SANDIA REPORT
SAND2005-7951
Unlimited Release
Printed January 2006

Cell-Directed Assembly of an Integrated Nanoelectronic/Nanophotonic Device for Probing Cellular Responses on the Nanoscale

Eric C. Carnes, Carlee E. Ashley, Helen K. Baca, DeAnna M. Lopez, Darren R. Dunphy, D. Bruce Burckel, Seema Singh, David R. Tallant, Regina L. Simpson, Hongyou Fan, and C. Jeffrey Brinker

Prepared by
Sandia National Laboratories
Albuquerque, New Mexico 87185 and Livermore, California 94550

Sandia is a multiprogram laboratory operated by Sandia Corporation,
a Lockheed Martin Company, for the United States Department of Energy's
National Nuclear Security Administration under Contract DE-AC04-94AL85000.

Issued by Sandia National Laboratories, operated for the United States Department of Energy by Sandia Corporation.

Available to DOE and DOE contractors from
U.S. Department of Energy
Office of Scientific and Technical Information
P.O. Box 62
Oak Ridge, TN 37831

Telephone: (865) 576-8401
Facsimile: (865) 576-5728
E-Mail: reports@adonis.osti.gov
Online ordering: http://www.osti.gov/bridge

Available to the public from
U.S. Department of Commerce
National Technical Information Service
5285 Port Royal Rd.
Springfield, VA 22161

Telephone: (800) 553-6847
Facsimile: (703) 605-6900
E-Mail: orders@ntis.fedworld.gov
Online order: http://www.ntis.gov/help/ordermethods.asp?loc=7-4-0#online

SAND2005-7951
Unlimited Release
Printed January 2006

Cell-Directed Assembly of an Integrated Nanoelectronic/Nanophotonic Device for Probing Cellular Responses on the Nanoscale

Eric C. Carnes[a], Carlee E. Ashley[a], Helen K. Baca[a], DeAnna M. Lopez[a], Darren R. Dunphy[b], D. Bruce Burckel[b], Seema Singh[b], David R. Tallant[c], Regina L. Simpson[c], Hongyou Fan[b], and C. Jeffrey Brinker[a,d]

[a]Chemical and Nuclear Engineering Department, Center for Micro-Engineered Materials, University of New Mexico, Albuquerque, NM 87106

[b]Ceramic Processing and Inorganic Materials Department, Sandia National Laboratory, P.O. 5800, Albuquerque, NM 87185-1349

[c]Materials Characterization Department, Sandia National Laboratory, P.O. 5800, Albuquerque, NM 87185-1411

[d]Self-Assembled Materials Department
Sandia National Laboratory, P.O. 5800, Albuquerque, NM 87185-1349

Abstract

Our discovery that the introduction of living cells (*Saccharomyces cerevisiae)* alters dramatically the evaporation driven self-assembly of lipid-silica nanostructures suggested the formation of novel bio/nano interfaces useful for cellular interrogation at the nanoscale. This one year "out of the box" LDRD focused on the localization of metallic and semi-conducting nanocrystals at the fluid, lipid-rich interface between *S. cerevisiae* and the surrounding phospholipid-templated silica nanostructure with the primary goal of creating Surface Enhanced Raman Spectroscopy (SERS)-active nanostructures and platforms for cellular integration into electrode arrays. Such structures are of interest for probing cellular responses to the onset of disease, understanding of cell-cell communication, and the development of cell-based bio-sensors. As SERS is known to be sensitive to the size and shape of metallic (principally gold and silver) nanocrystals, various sizes and shapes of nanocrystals were synthesized, functionalized and localized at the cellular surface by our 'cell-directed assembly' approach. Laser scanning confocal microscopy, SEM, and *in situ* grazing incidence small angle x-ray scattering (GISAXS) experiments were performed to study metallic nanocrystal localization.

Preliminary Raman spectroscopy studies were conducted to test for SERS activity. Interferometric lithography was used to construct high aspect ratio cylindrical holes on patterned gold substrates and electro-deposition experiments were performed in a preliminary attempt to create electrode arrays. A new printing procedure was also developed for cellular integration into nanostructured platforms that avoids solvent exposure and may mitigate osmotic stress. Using a different approach, substrates comprised of self-assembled nanoparticles in a phospholipid templated silica film were also developed. When printed on top of these substrates, the cells integrate themselves into the mesoporous silica film and direct organization of the nanoparticles to the cell surface for integration into the cell.

Acknowledgements

This work was partially supported by Sandia National Laboratory's Laboratory Directed R&D program and the Air Force Office of Scientific Research grant FA9550-04-1-0087. Confocal microscopy images were generated in the UNM Cancer Center Fluorescence Microscopy Facility which received support from NCRR 1 S10 RR14668, NSF MCB9982161, NCRR P20 RR11830, NCI R24 CA88339, NCRR S10 RR19287, NCRR S10 RR016918, the University of New Mexico Health Sciences Center, and the University of New Mexico Cancer Center. SEM images were performed at UNM's Center for Micro-Engineering on equipment funded by a NSF New Mexico EPSCoR grant. TEM studies were performed in the Department of Earth and Planetary at UNM. GISAXS was performed at the Advanced Photon Source at Argonne National Laboratory, supported by the U.S. Department of Energy, Office of Science, Office of Basic Energy Sciences, under Contract No. W-31-109-Eng-38.

Contents

Figures

Introduction

The integration of biological building blocks into functional platforms is important to applications across the field of nanotechnology (*1*). However, hybrid materials that incorporate biological units such as whole cells require functional bio/inorganic interfaces (*2-4*), benign synthesis conditions (*5-12*) and fluidic support systems to avoid dehydration (13). Cell-directed assembly integrates biological materials in a uniformly nanostructured inorganic host that maintains cell accessibility, addressability, and viability in the absence of an external fluidic architecture.

As we have reported earlier (*14*), during immobilization of *S. cerevisiae* cells in a porous, lipid-templated silica matrix utilizing evaporation-induced self-assembly, the cell forms its own novel interface through which it both directs assembly of the inorganic host phase and provides a fluid, membrane-like environment for the localization of proteins and nanocrystals in extended nanostructures. Characterization of the assembly process and the bio/nano interface through *in-situ* grazing incidence small angle X-ray scattering (GISAXS) (*15*), electron microscopy, and laser scanning confocal imaging, shows the cells profoundly alter the self-assembly pathway, creating around themselves multilayered phospholipid vesicles that interface coherently with the nanostructured silica host. The immobilized cells mediate their local pH and stress, collectively switching the silica mesophase. Replacing the cell with several cell models demonstrates that the living cell is necessary for the formation of the lipid interface and transformation of the inorganic phase, serving as a site for lipid aggregate nucleation and ordering. The living cell's response to osmotic stress is an important part of its ability to direct the structure of its local and global environments. Cell-directed assembly supports a highly biocompatible immobilization strategy that extends viability of immobilized cells to several weeks and creates cell-directed hierarchical structures that serve as stand-alone sensors through reporter protein expression, or organize proteins and nanocrystals at the cell surface. The cell's ability to organize ordered assemblies of lipids, mediate its local chemical and physical environment, and form a seamless bio/nano interface suggests that cell-directed assembly represents a new general synthetic approach wherein cells direct their self-integration into functional multiscale nano/bio devices.

One way to exploit this new interface is by utilizing Surface Enhanced Raman Spectroscopy (SERS). In SERS, Raman signals can be enhanced by many orders of magnitude

(>10^4) due to the high local optical fields of metallic nanostructures. Ideal SERS-active metallic nanostructures are aggregates of 3-100-nm diameter gold or silver nanoparticles. Optical field enhancement occurs due to resonances of the applied optical field with surface plasmon oscillations of the metallic nanostructure. Given the addition of these nanoparticles during the cell-directed assembly process, a metallic nanostructure can be developed around each cell, which should allow sensitive spectroscopic probing of the cell surface. Over time, nanocrystals (NCs) enter the cell where they should continue to serve as local probes of molecular structure – especially in the vicinity of nanocrystal aggregates that appear to form within the cells. As spectra can be acquired in seconds, it should be possible to follow in real time structural transformations that accompany/allow NC entrance into the cell. Bio-conjugation of the NCs with molecular receptors could be used to target NC attachment to specific cellular components. Comparison with control (non-conjugated) NC systems should allow identification of molecular recognition events, possibly enabling determination of the onset of infection.

I. The Bio/Nano Interface via Cell-directed Assembly

Following our group's recent discovery of the remarkable ability for living cells to incorporate themselves as part of the evaporation-induced self assembly process, it was quickly discovered that the cells are also able to organize bio-compatible, functionalized nanocrystals during the drying process. Our group has also previously demonstrated how to make bio-compatible nanocrystals in an efficient and direct manner (*16*). A schematic of the bio/nano interface formed via cell-directed assembly process utilizing bio-compatible nanoparticles has been illustrated in Figure 1.

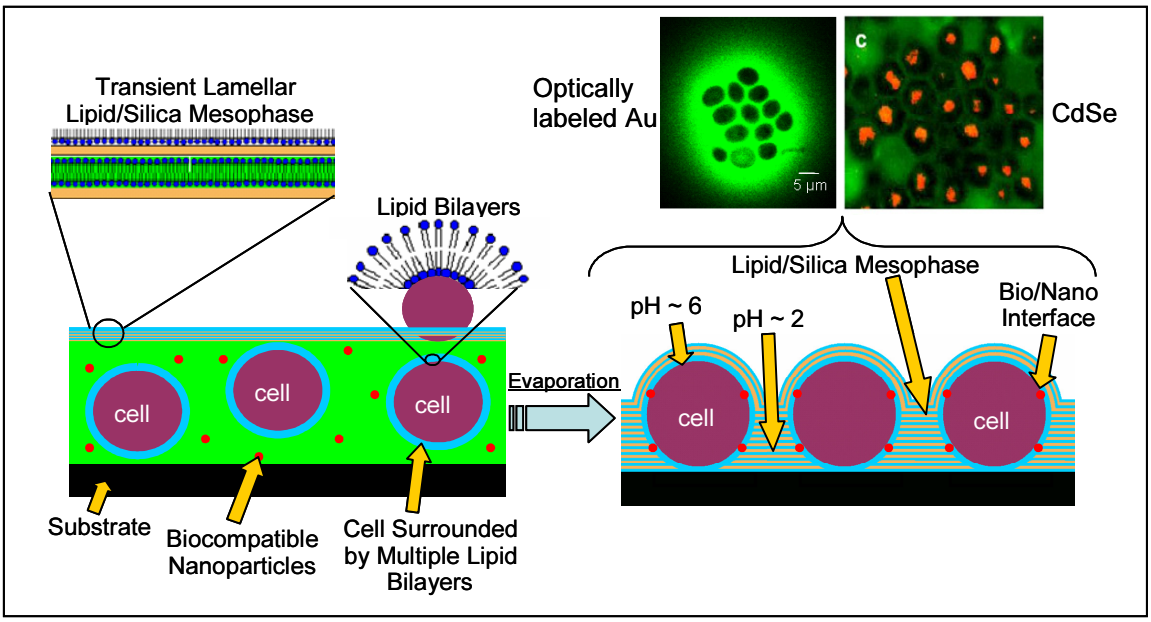

Figure 1. Schematic illustration of the formation of a functional bio/nano interface formed via cell-directed assembly

To study NC localization scanning electron microscopy (SEM), transmission electron microscopy (TEM), GISAXS, and, for optically labeled NCs, fluorescence microscopy and confocal laser-scanning microscopy were used. These studies, although limited in the scope of the functionalization chemistry, suggested that phospholipid functionalization is necessary for cellular localization. As can be seen in Figure 2, TEM images employing 2-nm gold nanocrystals show that, during evaporation-induced self-assembly of lipid/silica nanostructures incorporating *S cerevisiae*, gold NCs are localized at the cellular surface forming the bio/nano interface. Figure 3 displays SEM studies performed with energy dispersive electron spectroscopy (EDS) confirmed fluorescence microscopy results that show gold NC localization at the immediate surface of the cell.

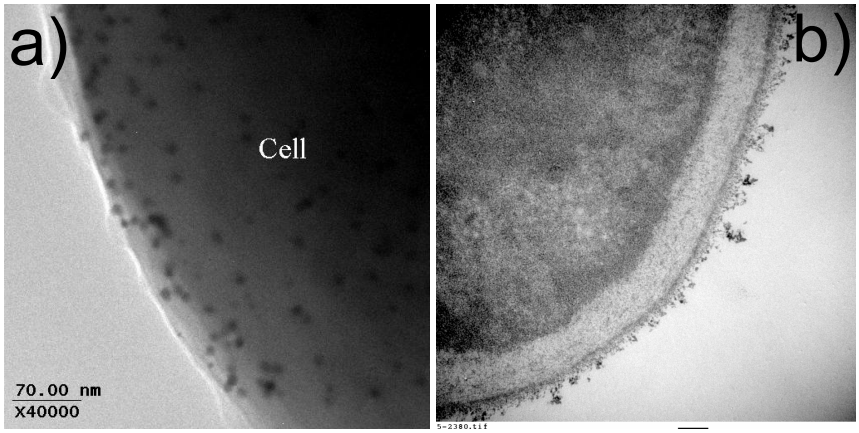

Figure 2. TEM images of gold NCs at the surface of a cell forming the bio/nano interface, a) top view, b) cross-section

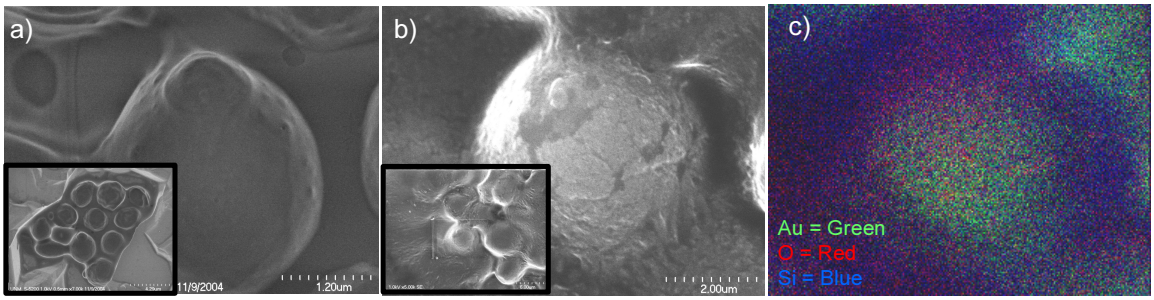

Figure 3. a) SEM image of cells in a silica film immobilized utilizing cell-directed assembly, b) SEM image of gold NCs on the surface of an immobilized cell, c) 2-D EDS spectra of image b clearly showing the presence of gold NCs

As NC localization could allow the formation of a SERS-active nanostructure that might be operative even during internalization, this project focused on extending the initial work to create SERS-active structures in which living cells and NCs are immobilized in a nanostructured fluidic architecture. Interestingly, GISAXS studies indicate that NC localization can in some cases result in ordered NC arrays at the cellular surface, as can be seen in Figure 4. Such arrays, if proven to be SERS-active, could be precisely tuned with respect to particle spacing – perhaps allowing optimization of the SERS-active nanostructure.

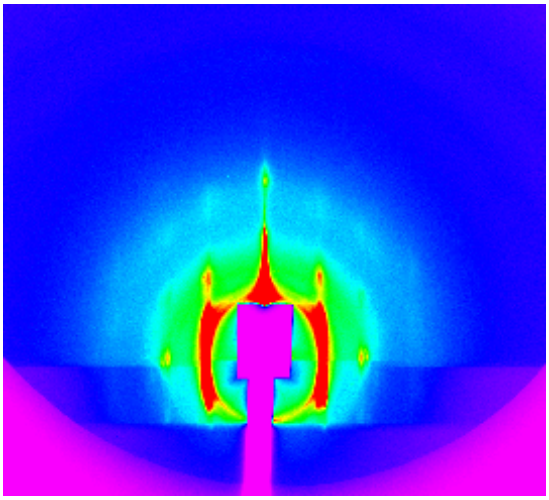

Figure 4. GISAXS of cells with 2 nm lipid-coated gold particles in a silica film formed via cell-directed assembly

II. Surface Enhanced Raman Spectroscopy

Having confirmed cell-directed NC localization at the cell surface, attempts were made to obtain SERS-enhanced spectra. Raman spectra were obtained using argon (514 nm) and krypton (647 nm) ion laser lines. The films were illuminated though an optical microscope (approximately 1 um horizontal resolution) coupled to a triple spectrograph with a liquid nitrogen cooled, charge-coupled-device detector. The spectra obtained of the immobilized cell films have significant backgrounds of broad features due to fluorescence. These broad features were removed from the spectra by a fitting procedure for presentation in this report. However, the overall levels of Raman scatter are low, so that relatively high noise levels and a few artifacts related to the fitting procedure (e.g., features with downward-pointing peaks) remain in the spectra.

Figure 5 shows Raman spectra, obtained with 647 nm excitation, of films created by cell-directed assembly. It was hoped that intimate contact of the gold would result in enhancement of Raman scatter from components of the yeast cells by the SERS effect. The spectra from two locations on the film in which gold is present show significantly more intense Raman bands (due to $-CH_2-$, from alkane chains) than the spectrum from the film which lacks the gold NCs. Also, a band due to carboxylate groups, probably from neutralized organic acids, is present only in the

spectra of the gold NC-containing film. The polar nature of carboxylate groups means that they have a relatively high probability of coupling to the gold NCs, thereby increasing the likelihood of SERS effects. However, the intensity increase of the Raman bands from the gold NC-containing films corresponds to a very modest SERS effect.

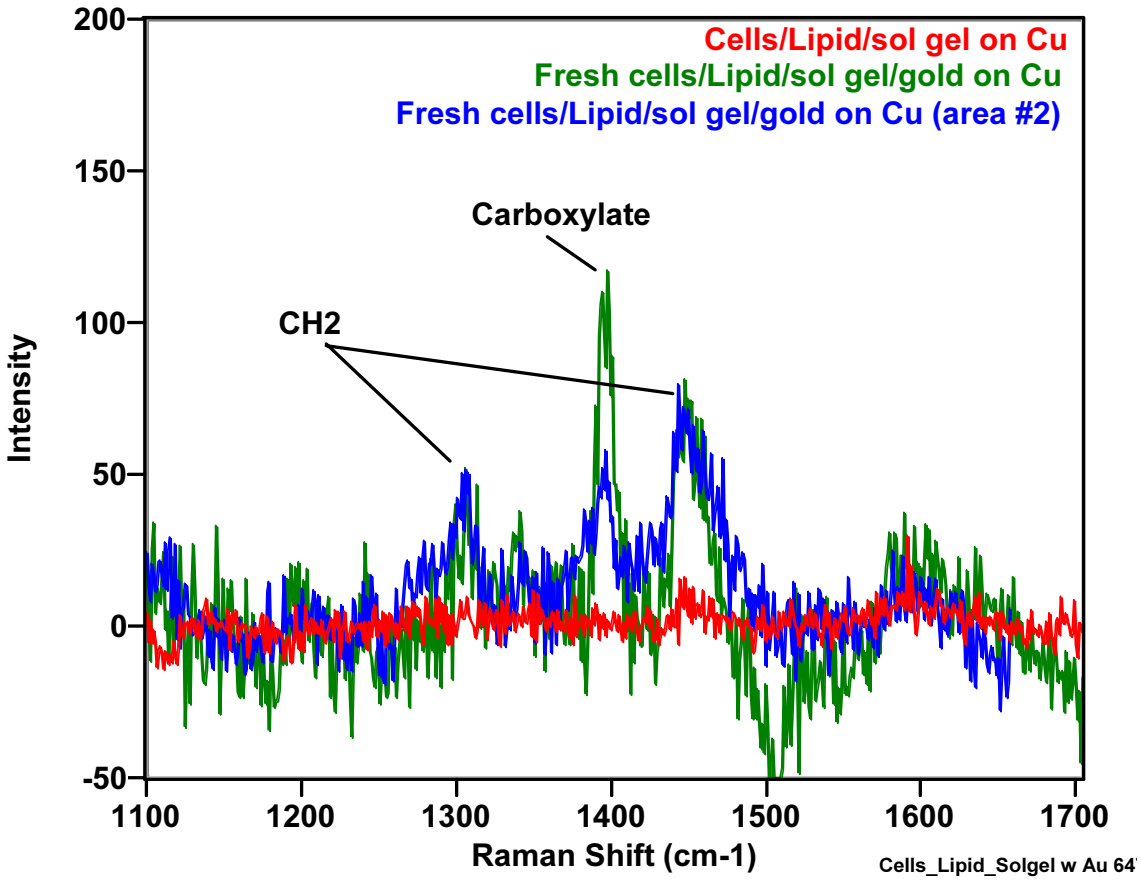

Figure 5. Raman spectra, obtained with 647 nm excitation, of cells immobilized via cell-directed assembly on copper, plus gold NC

As SERS is inherently sensitive to both sample preparation (e.g. size and concentration of NCs) and operating conditions (e.g. excitation wavelength), the lack of access to a dedicated Raman spectrometer has seriously hindered progress in this area. Collaborative experiments with UC Santa Cruz have yielded non-reproducible results – presumably due to the limited numbers of experiments, the heterogeneous nature of our samples (cell-containing regions separated by silica nanostructures), and the sensitivity of SERS to sample processing and experimental parameters. Recent experiments performed at Sandia have resulted in Raman spectra of samples containing

cells with and without localized nanocrystals. However, further tests are needed both to confirm the SERS enhancement of these spectra as well as to optimize the parameters for performing SERS.

III. Creation of SERS-optimized Bio-Compatible Nanoparticles

SERS is known to be sensitive to the size, shape and composition of the metallic nanoparticles. Optimum nanoparticles are gold or silver with diameters of 20-100 nm and having a shape that provides maximum surface area. Our initial work employed 2-3-nm gold NCs, thus we adapted literature procedures to synthesize larger silver NCs (30 nm spheres) and low-aspect ratio, gold nanorods (80 x 40 nm) (*17*), both of which are known to be highly SERS-active. TEM images of these SERS-active particles are shown in Figure 6.

Surface functionalization is important in directing NC localization. For our initial studies using 2-3 nm gold NCs, we modified the initially hydrophobic alkanethiol terminated surfaces with phospholipids (and optically-labeled phospholipids), creating a hybrid bilayer that made the NCs water soluble and directed their localization. Similar procedures were used for hydrophobic oleylamine-terminated silver NCs. Gold nanorods however are prepared in aqueous solvents with cetyltrimethylammonium bilayer terminated surfaces. No satisfactory process has been developed to date to functionalize these nanoparticles with phospholipids.

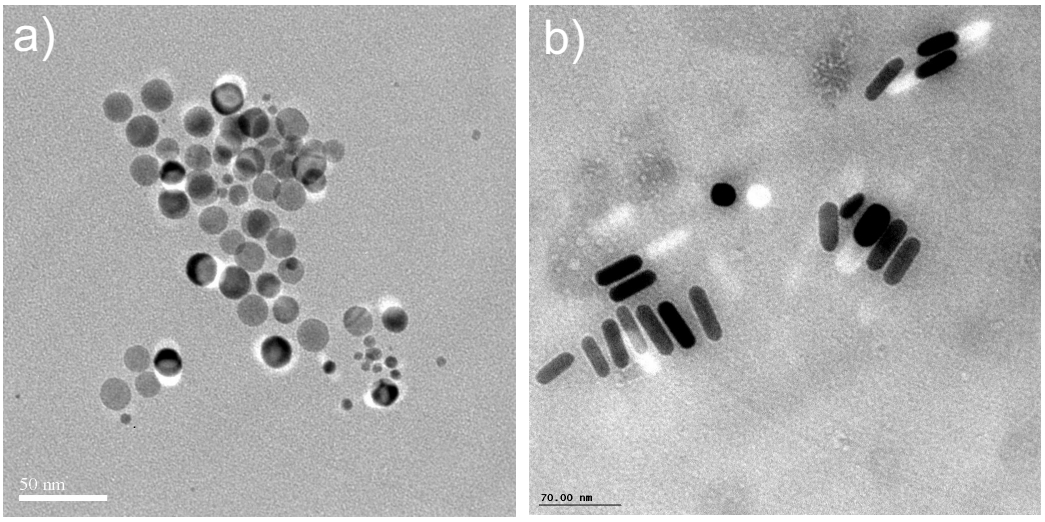

Figure 6. TEM images of a) 30 nm lipid-coated silver nanoparticles, and b) 80 x 40 nm water-soluble gold nanorods

IV. Fabrication of Nanoelectrodes

A concurrent task of this project was the construction of a substrate containing small, high aspect ratio gold posts for use as electrodes – the idea being that cells would recognize and internalize lipid-coated gold posts, thereby integrating themselves into an electronic platform. Fabrication of high aspect ratio metallic structures is complicated by several factors. First, there are inherent limits on lithography of high aspect ratio features in photoresist such as resist resolution, mechanical stability, exposure wavelength and diffraction. Second, given a high aspect ratio hole in photoresist, filling the hole with metal is difficult. Approaches such as sputtering or metal evaporation are prone to clogging the opening to the hole prior to complete "via" fill. Given typical cell dimensions, the initial design specifications were to fabricate gold pillars approximately 50 nm in width and 5 μm in height, an aspect ratio of 100. Such a demanding aspect ratio is clearly beyond the capability of current lithography, prompting us to devise a three pronged approach to achieve our goal. The first step is to optimize the lithography process to attain the highest aspect ratio features possible. The second fabrication choice was to opt for a "bottom up" via fill approach -- electrochemical deposition of gold. The final step is to take the highest aspect ratio electrodeposited gold post and post-fabrication etch-back to yield the final cell probe structure. In this final step, the aspect ratio of the post is improved due to the isotropic nature of the etch-back. The radius of the post shrinks relative to its height.

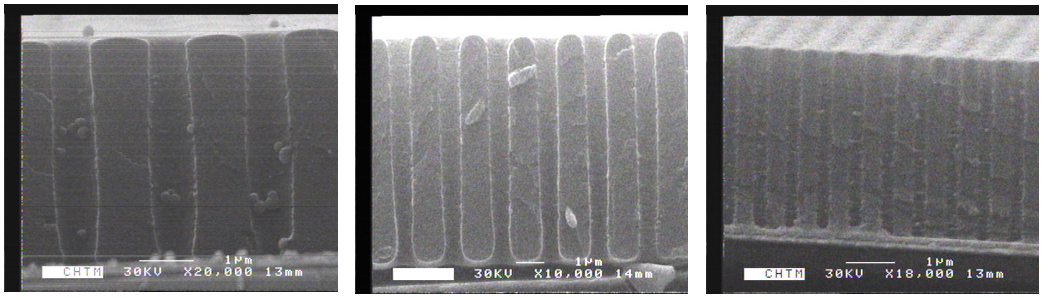

Figure 7. a) Hole array in SU-8 with aspect ratio ~3, b) Hole array in SU-8 with aspect ratio ~9, and c) Hole array in SU-8 with aspect ratio ~14.

Initial work on the high aspect ratio lithography focused on using interferometric lithography (IL) and the SU-8 negative tone photoepoxy resist system. A frequency tripled Nd:YAG laser in the Lloyd mirror configuration was used to generate 1-D interference patterns.

Consecutive exposures were then used to expose 2-D hole-arrays in the SU-8 photoepoxy. Optimization of the angle of incidence, exposure dose, post-exposure bake time and temperature, and develop times, yielded hole-arrays with high aspect ratios. Figure 7 shows some representative examples along the optimization path, with aspect ratios of ~3, ~9 and ~14. In the final device, hole arrays over the entire substrate are not desired, in which case, a mix-and-match photolithography approach will be pursued. Photoresist exposure is an additive process, so that conventional lithography can be used to selectively expose the resist, yielding IL-generated holes only in the desired location.

For safety and environmental reasons, a non-cyanide based gold electrochemical deposition bath was chosen (that utilizes complexation and reduction of Au(III) by thiosulfate to form stable plating solutions) (18). The pH of the plating bath was found to be a critical parameter for solution stability; if the pH was not adjusted immediately to ca. 7.4 after dissolution of the bath ingredients, precipitation of gold occurred within a few minutes. At pH 7.4, the bath appeared stable for several hours. Deposition was performed using a constant current of 10 mA/cm^2 onto platinum substrates (other metal substrates, including chromium, silver, and nickel yielded films of inferior quality). Figure 8a shows a cross section SEM photograph of an apparently partially filled SU-8 hole array. Figure 8b shows a similar cross section SEM indicating that the gold posts filling the vias suffer from poor morphology, and are in many cases, hollow. The cause for this poor morphology has yet to be determined, but is surely influenced by the complex surface chemistry between the plating bath and the SU-8 resist surface.

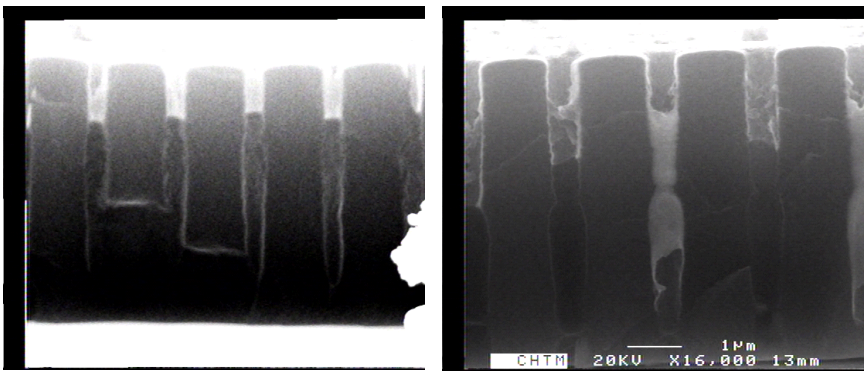

Figure 8. a) Cross-section SEM showing partially filled hole array, b) Cross-section SEM showing hollow gold post inside hole array.

Being a photocurable epoxy, SU-8 is typically used in applications where it is intended to remain behind as part of the ultimate device. Under standard processing conditions, fully cross-linked and thermally treated SU-8 is difficult to remove. However, the processing conditions used to generate the high aspect ratio features seen above lie outside these usual processing conditions, resulting in partially cross-linked resist. Delamination and removal of the partially cross-linked resist occurs under prolonged exposure to the SU-8 developer. The SEM images in Figure 9 demonstrate several issues with this approach. From the top-down image of the substrate after resist removal in Figure 9a, it is apparent that the film suffered from non-uniform filling of the hole array. This is most likely due to incomplete resist removal in the bottoms of the holes, and can be addressed by resist process modifications such as extending the develop time slightly. The SEM of the surface in Figure 9b is more problematic. Here it is apparent that the deposited posts were broken and removed with the SU-8 resist film. This is confirmed by the SEM of a portion of SU-8 after removal from the substrate in Figure 9c. Gold posts remain in some of the holes of the SU-8 film. This image also shows further evidence of hollow gold posts, as several of the gold posts have a void in the center, resulting in an annular appearance.

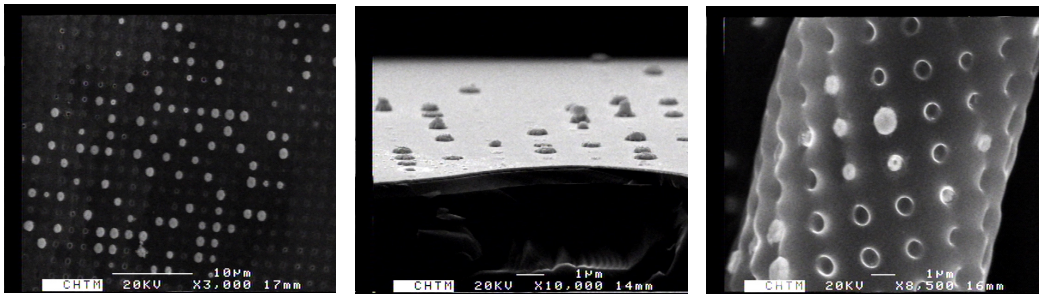

Figure 9. a) Top down SEM showing incomplete hole array, b) SEM showing of surface showing broken gold posts, c) SEM of SU-8 film after removal indicating broken posts in film as well as void in the center of the hollow posts.

The tendency of the SU-8 film combined with the plating bath chemistry to produce hollow posts is promising, however the mechanism is not understood, and the observation could be the result of any number of parameters. Perhaps the more challenging issue is the tendency of the SU-8 film to break off the filled posts during resist removal. So, while the SU-8 is capable of resolving very high aspect ratio features, these initial results seem to indicate a change in course

to a less rugged resist is warranted. Along this path, some exploratory work with an image reversible resist, AZ 5214, was performed. Image reversible resists function as positive resists under normal process conditions, but switch to negative tone when a post-exposure bake, and flood exposure are performed after initial pattern exposure. Figure 10 shows the initial results, demonstrating much lower aspect ratio as well as significant side wall curvature, indicating that this resist system is probably ill-suited for our needs. Future directions for the fabrication of the nanoelectrodes include exploring thick, conventional photoresists capable of being chemically dissolved rather than physically removed, as well as use of more stable plating baths.

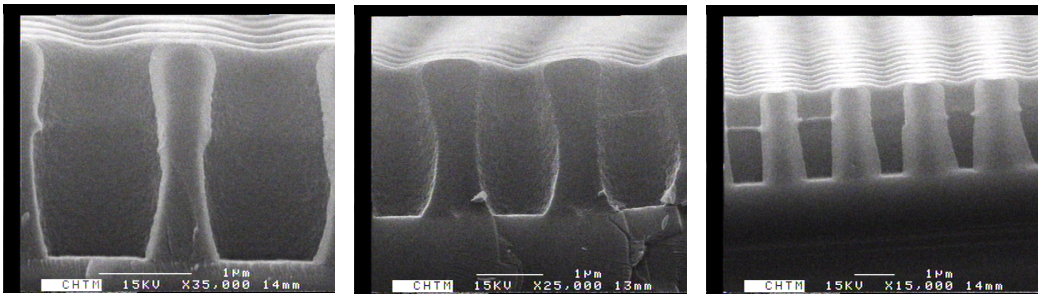

Figure 10. a) Top down SEM showing incomplete hole array, b) SEM showing of surface showing broken gold posts, and c) SEM of SU-8 film after removal indicating broken posts in film as well as void in the center of the hollow posts.

V. Cellular Patterning and Integration onto Substrates

Using a different approach to create biocompatible substrates that would allow for cellular integration, substrates comprised of self-assembled nanoparticles in a phospholipid-templated silica film were also developed. In this novel technique, when printed on top of these substrates, the cells can actually integrate themselves into the mesoporous silica film and direct organization of the nanoparticles to the cell surface for integration into the cell, as illustrated in the schematic in Figure 11.

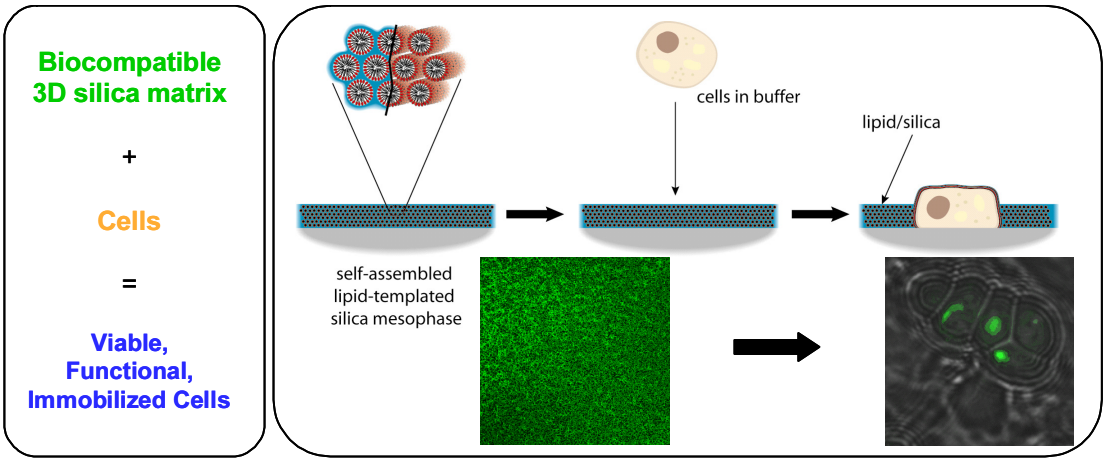

Figure 11. Schematic of cellular integration into a bio-compatible silica film

First, a bio-compatible mesoporous silica template containing functionalized nanoparticles is made using evaporation-induced self-assembly. Cells are then introduced on top of the dry silica film. The cells then rehydrolyze and condense the surrounding silica film, returning the system to a state of quasi-fluidity. In this state the cell can organize its environment in a manner similar to that of cell-directed assembly, yielding a fully functional cell immobilized in a porous, 3D silica mesophase. An SEM image of a cell introduced on top of a bio-compatible silica film can be seen in Figure 12.

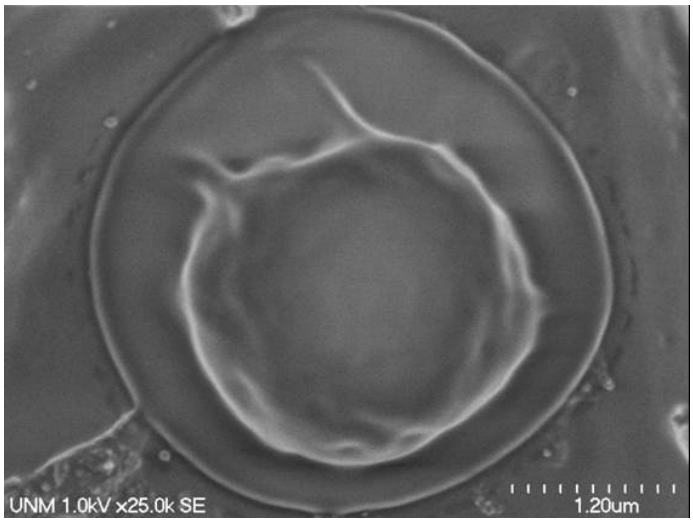

Figure 12. A cell that has integrated itself into a bio-compatible mesoporous silica film

As seen by the localization of optically-labeled gold NC in Figure 13, the cell can also organize lipids and bio-compatible nanoparticles in its vicinity, followed by drying and recondensation of the silica matrix to yield immobilized cells that maintain many of the same properties as those found using the cell-directed assembly approach. This approach, however, may provide an even better route for bio-compatible cell immobilization as it could minimize many undesired effects of having the cell present during the evaporation-induced self-assembly process. For example, the cell would no longer have to be exposed directly to alcohols and acids or bases. Additionally, the osmotic stresses on the cell associated with the evaporation process may be greatly reduced. Future directions for this novel cell integration technique involve patterning of the cells on the mesoporous silica substrates. This could be accomplished using ink-jet printing to dispense cells on top of a pre-existing film according to a desired template to create functional cellular arrays.

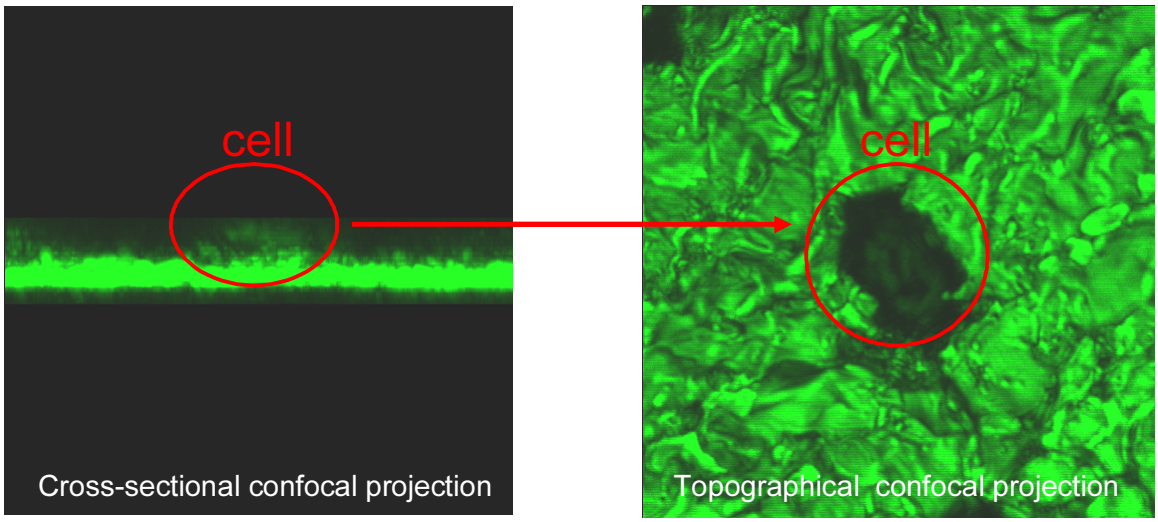

Figure 13. Confocal images showing the localization of optically-labeled gold NC by cells placed on top of a bio-compatible silica film containing the gold NC

References

1. S. G. Zhang, *Nature Biotechnology* 22, 151-152 (2004).
2. M. Tirrell, E. Kokkoli, M. Biesalski, *Surface Science* 500, 61-83 (2002).
3. R. Langer, D. A. Tirrell, *Nature* 428, 487-92 (2004).
4. R. F. Service, *Science* 297, 962-963 (2002).
5. E. Pope, *Journal of Sol-Gel Science and Technology* 4, 225-229 (1995).
6. S. Y. Chia, J. Urano, F. Tamanoi, B. Dunn, J. I. Zink, *Journal of the American Chemical Society* 122, 6488-6489 (2000).
7. J. R. Premkumar *et al.*, *Chemistry of Materials* 14, 2676-2686 (2002).
8. N. Nassif *et al.*, *Nature Materials* 1, 42-4 (2002).
9. A. Coiffier, T. Coradin, C. Roux, O. M. M. Bouvet, J. Livage, *Journal of Materials Chemistry* 11, 2039-2044 (2001).
10. J. F. T. Conroy *et al.*, *Journal of Sol-Gel Science and Technology* 18, 269-283 (2000).
11. I. Gill, A. Ballesteros, *Journal of the American Chemical Society* 120, 8587-8598 (1998).
12. L. Inama, S. Dire, C. G., A. Cavazza, *Journal of Biotechnology* 30, 197-210 (1993).
13. M. L. Ferrer, L. Yuste, F. Rojo, F. del Monte, *Chemistry of Materials* 15, 3614-3618 (2003).
14. C. Brinker, Y. Lu, A. Sellinger, H. Fan, *Advanced Materials* 11, 579-+ (1999).
15. D. A. Doshi *et al.*, *Journal of the American Chemical Society* 125, 11646-11655 (2003).
16. H. Y. Fan *et al.*, *Science* 304, 567-571 (2004).
17. C.J. Orendorff *et al.*, *Analytical Chemistry* 77, 3261-3266 (2005).
18. Green TA, Liew MJ, Roy S, *Journal of the Electrochemical Society*, 150 (3) C104-110 (2003)

Appendix -- Publications and Presentations

1. *Developing Complex Structures and Functions Through Cell-Directed Assembly*, Helen K. Baca, PhD Dissertation, the University of New Mexico, Department of Chemical and Nuclear Engineering (July 2005)

2. *Cell-Directed Assembly of the 3-D Bio-Nano Interface,* Helen K. Baca, Eric C. Carnes, Carlee E. Ashley, DeAnna Lopez, Seema Singh, and C. Jeffrey Brinker, Materials Research Society Multifunctional Ceramic Composites Workshop, Urbana, IL (October 2005)

3. *Cell-Directed Assembly of 3-D Bio-Nano Interfacse,* Helen K. Baca, Carlee E. Ashley, Eric C. Carnes, DeAnna Lopez, Seema Singh, and C. Jeffrey Brinker, 18th Annual NSF/EPSCoR National Conference, San Juan, Puerto Rico (September 2005)

4. *Bio-inspired Self-Assembly of Multifunctional Porous and Composite Nanostructures,* C. Jeffrey Brinker, INVITED, AFOSR Workshop on Multifunctional Materials, Keystone, CO (August 2005).

5. *Complex Structures and Functions Through Cell-Directed Assembly,* Helen K. Baca, Carlee E. Ashley, Eric C. Carnes, Seema Singh, and C. Jeffrey Brinker, 13th International Workshop on Sol-Gel Science and Technology, Los Angeles, CA (August 2005).

6. *The Development of Complex, Functional Structures Through Cell-Directed Self-Assembly,* Helen K. Baca, Eric C. Carnes, Carlee E. Ashley, DeAnna Lopez, and C. Jeffrey Brinker, 2005 Users Meeting for the Advanced Photon Source and the Center for Nanoscale Materials (May 2005).

7. *Developing Complex Structures and Functions Through Cell-Directed Self-Assembly,* Helen K. Baca, Carlee E. Ashley, Eric C. Carnes, DeAnna Lopez, and C. Jeffrey Brinker, Materials Research Society Spring Meeting, San Francisco, CA (April 2005).

8. *Cell-Directed Assembly of the Bio-Nano Interface,* INVITED*,* Helen K. Baca, Carlee E. Ashley, Eric C. Carnes, DeAnna Lopez, Seema Singh and C. Jeffrey Brinker, Materials Research Society Spring Meeting, San Francisco, CA (April 2005).

9. *Evaporation-Induced Self-Assembly of Porous, Composite and Biocompatible Thin Film Nanostructures,* INVITED*,* C. Jeffrey Brinker, 229th American Chemical Society Meeting, San Diego, CA (March 2005).

10. *Bio-inspired Self-Assembly of Porous and Composite Nanostructures,* C. Jeffrey Brinker, INVITED, AAAS Annual Meeting, Washington, DC (February 2005).

11. *Bio-inspired Self-Assembly of Porous and Composite Nanostructures,* C. Jeffrey Brinker, AFOSR Biomimetics, Biomaterials and Biointerfacials Sciences Program Review, San Diego, CA (January 2005).

Distribution

1	MS1349	Eric C. Carnes, 1815
1	MS1349	Carlee E. Ashley, 1815
1	MS1349	Helen K. Baca, 1815
1	MS1349	DeAnna M. Lopez, 1815
1	MS1349	Darren R. Dunphy, 1815
1	MS1349	D. Bruce Burckel, 1815
1	MS1349	Seema Singh, 1815
1	MS1349	Hongyou Fan, 1815
1	MS1411	David R. Tallant, 1822
1	MS1349	Regina L. Simpson, 1822
1	MS1349	C. Jeffrey Brinker, 1002
4	MS1349	Carol S. Ashley, 1815
2	MS9018	Central Technical Files, 8945-1
2	MS0899	Technical Library, 4536
1	MS0161	Patent and Licensing, 11500
1	MS0123	D. Chavez, LDRD Program, 1011


Sandia National Laboratories